PTEP

Prog. Theor. Exp. Phys. **2022** 123H01(12 pages)
DOI: 10.1093/ptep/ptac157

Emission characteristics of gadolinium ions in a water Cherenkov detector

Y. Iwata[1,2], H. Sekiya[3,4], and C. Ito[5]

[1]*Advanced Radiation Measurement and Analysis Research Group, Collaborative Laboratories for Advanced Decommissioning Sciences, Japan Atomic Energy Agency, 2-4 Shirakata, Tokai-mura, Naka-gun, Ibaraki 319-1195, Japan.*
[2]*Nuclear Professional School, The University of Tokyo, 2-22 Shirakata-Shirane, Tokai-mura, Naka-gun, Ibaraki 319-1188, Japan*
[3]*Kamioka Observatory, Institute for Cosmic Ray Research, The University of Tokyo, 456 Higashi-Mozumi, Kamioka, Hida, Gifu 506-1205, Japan*
[4]*Kavli Institute for the Physics and Mathematics of the Universe (WPI), The University of Tokyo Institutes for Advanced Study, The University of Tokyo, Kashiwa, Chiba 277-8583, Japan*
[5]*Experimental Fast Reactor Department, Oarai Research and Development Institute, Japan Atomic Energy Agency, 4002 Narita, Oarai, Ibaraki 311-1393, Japan*
*E-mail: iwata.yoshihiro@jaea.go.jp

Received August 26, 2022; Revised November 16, 2022; Accepted November 25, 2022; Published November 28, 2022

To observe supernova relic neutrino events, 13 tons of gadolinium sulfate octahydrate ($Gd_2(SO_4)_3{\cdot}8H_2O$), corresponding to 0.01% Gd solution, was dissolved in the Super-Kamiokande water Cherenkov detector in 2020. The aim is to improve the detection efficiency of neutrons from inverse β decay involving electron antineutrinos. However, Gd^{3+} ions can be excited by the Cherenkov light from cosmic muons, and the subsequent emission at 312 nm is a possible background (BG) source for Cherenkov signal detection. In this work, we constructed an experimental setup based on time-resolved laser-induced luminescence spectroscopy to investigate the emission characteristics of Gd^{3+} ions in water. The excitation laser wavelength was tuned in the range of 245–255 nm, and large resonant peaks were observed at 246.2 nm and 252.3 nm with measured emission lifetimes of around 3 ms. Good linearity was observed between Gd concentration and emission intensity for these two wavelengths, indicating that our setup is useful for remote monitoring of Gd concentration. According to the simulation results using our spectroscopic data and reference values, the Gd^{3+} emission BG rate from cosmic muons is expected to be 10^{-1} counts/μs or less, which seems small but not negligible.

Subject Index H20

1. Introduction

Gadolinium (Gd) is a rare earth metal belonging to the lanthanide series. It usually exists as a trivalent ion (Gd^{3+}) with the $4f^7$ electronic configuration in aqueous solution. Due to this stable half-filled shell configuration, the lowest excited level ($^6P_{7/2}$) of Gd^{3+} has exceptionally high energy (wavenumber of $>32\,000$ cm^{-1}) compared to other lanthanide ions [1–3]. One of the main characteristics of Gd is its large neutron absorption cross section. Of the seven stable isotopes, ^{157}Gd is a strong neutron absorber (thermal neutron capture cross section of 2.54×10^5 barn), which can be used as soluble neutron poison for nuclear criticality control in nuclear fuel cycle facilities [4]. Thermal neutron absorption by Gd results in the emission of an average

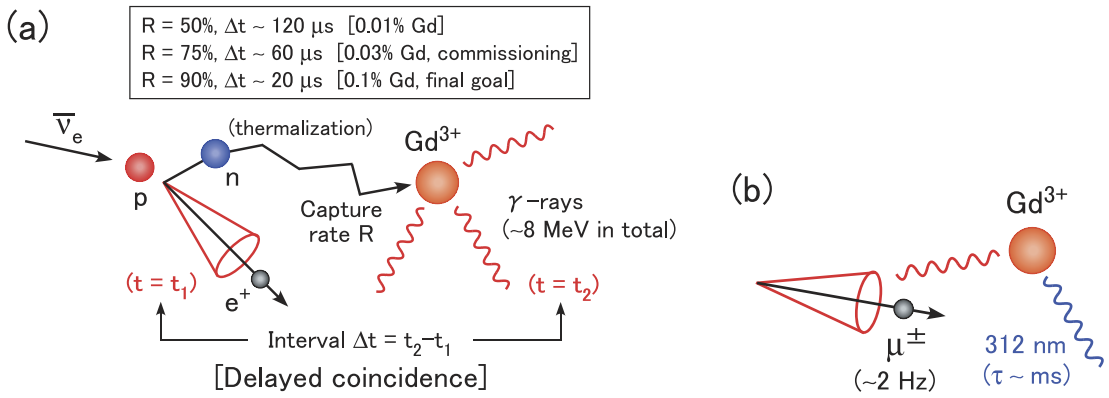

Fig. 1. (a) Principle of the delayed coincidence technique. (b) Expected Gd^{3+} emission background induced by the Cherenkov light from cosmic muons.

of three γ-rays with a total energy of 8 MeV, which is higher than 2.2 MeV in the case of the proton.

Because of the large cross section and high γ-ray energy of this (n, γ) reaction, it was proposed to add Gd to the Super-Kamiokande (SK) 50 kton water Cherenkov detector [5]. SK is a versatile detector covering the fields of particle physics and astroparticle physics. In particular, observing supernova relic neutrino (SRN) events is expected using the delayed coincidence between positron and neutron from inverse beta decay: $\bar{\nu}_e + p \rightarrow e^+ + n$. The aim of introducing Gd is to increase the detection efficiency of neutrons, and thereby improve the detection sensitivity of the electron antineutrino SRN events. Following the success of a feasibility study called the EGADS project [6], 13 tons of Gd sulfate octahydrate ($Gd_2(SO_4)_3{\cdot}8H_2O$, simply Gd sulfate in the following), corresponding to 0.01% Gd solution, was dissolved in the SK ultrapure water to start the SK-Gd project in August 2020 [7]. More recently, an additional 26 tons of Gd sulfate was dissolved to increase the Gd concentration to 0.03%. Figure 1(a) shows the principle of the delayed coincidence technique, where R and Δt represent the neutron capture rate by Gd^{3+} ions and the time interval between positron and γ-ray generation, respectively. The final goal of the SK-Gd project is $(R, \Delta t) \sim (90\%, 20\,\mu s)$ at a Gd concentration of 0.1%. Neutrons not captured by Gd either react with protons in water to emit γ-rays with an energy of 2.2 MeV, or escape the detector without any reaction. On the other hand, cosmic muons with an average energy of about 271 GeV penetrate the SK detector at a frequency of about 2 Hz [8,9]. Gd^{3+} ions can be excited by short-wavelength Cherenkov light from these muons, and the subsequent emission at 312 nm is a possible background (BG) source for the detection of Cherenkov signals, as shown in Fig. 1(b).

In this work, we construct an experimental setup based on time-resolved laser-induced luminescence spectroscopy to investigate the emission characteristics of Gd^{3+} ions in water. Also, a simulation study was performed assuming the geometry of the SK-Gd detector to estimate the influence of the Gd^{3+} emission BG on the detector.

2. Emission characteristics of Gd^{3+} ion

The emission lifetime of trivalent lanthanide ions is a typical parameter representing their emission characteristics. The observed lifetime τ_{obs} of the excited level is expressed by:

$$\tau_{obs} = 1/\left(k_{rad} + \sum k_{nr}\right), \quad (1)$$

where $k_{\rm rad}$ and $k_{\rm nr}$ are the radiative and non-radiative rate constants, respectively [10]. $k_{\rm nr}$ includes the quenching phenomenon by high-energy vibrations such as O–H (3600 $\rm cm^{-1}$) in water. Some literature values have been reported on the observed Gd^{3+} emission lifetime in the presence of perchlorate ions: $\tau_{\rm obs} = 2300\ \mu$s [10] and $1480 \pm 20\ \mu$s [11]. Compared to other adjacent lanthanide ions like Sm^{3+}, Eu^{3+}, Tb^{3+}, and Dy^{3+} with emission lifetimes of the order of μs–100 μs [12], the large energy gap $\Delta E > 32\,000\ \rm cm^{-1}$ of Gd^{3+} causes its relatively longer (∼ms) lifetime. A calculated radiative Gd^{3+} lifetime of $\tau_{\rm rad}(= 1/k_{\rm rad}) = 10.9$ ms has also been reported [13].

It is known that some inorganic anions, such as nitrate ions in aqueous solution, show strong quenching of the Gd^{3+} emission at 312 nm [14]. This quenching may help reduce the Gd^{3+} emission BG described in Sect. 1, but nitrate ions absorb a large portion of Cherenkov photons in the UV region [15–17]. Therefore, the chemical form of Gd sulfate instead of Gd nitrate ($Gd(NO_3)_3$) is used in the SK-Gd project to dissolve Gd in water [6,7]. Sulfate ions in an aqueous solution of Gd sulfate do not exhibit significant quenching or absorption with a Gd concentration in the range of 0.01–0.1%.

To evaluate the Gd^{3+} emission BG at the SK-Gd detector, the following optical properties of the Gd^{3+} ion are required: molar attenuation coefficients ϵ_i at resonant wavelengths λ_i with their full widths at half maximum (FWHMs) and a molar attenuation coefficient $\epsilon_{\rm DC}$ at non-resonant wavelengths shorter than the emission wavelength (312 nm). According to the Beer–Lambert law, the molar attenuation coefficient ϵ in $\rm mol^{-1}{\cdot}L{\cdot}cm^{-1}$ ($\rm M^{-1}{\cdot}cm^{-1}$ in the following; $\rm M \equiv mol/L$) has the following relationship with the transmittance T of light: $T = 10^{-\epsilon LC}$, where L in cm is the optical path length, and C in M is the molar concentration of Gd in water. A 0.1% Gd solution is equal to ∼0.006 374 M. The Gd^{3+} ion has a large absorption band at 272–278 nm, corresponding to the resonance excitation to ^6I_J levels [3,13], but the use of these strong absorption lines is considered unsuitable for quantitative analysis of Gd concentration in the range of 0.01–0.1%; the ratio of absorption at Gd concentrations of 0.01% and 0.1% with the maximum $\epsilon = 3.41\ \rm M^{-1}{\cdot}cm^{-1}$ and a typical sample cell length $L = 2$ cm is calculated to be:

$$\frac{\text{Absorption at 0.01\% Gd}}{\text{Absorption at 0.1\% Gd}} \sim \frac{1 - 10^{-3.41\times2\times0.000\,6374}}{1 - 10^{-3.41\times2\times0.006\,374}} \sim 0.105, \tag{2}$$

implying a systematic error of 5%. On the other hand, there is a moderate ($\epsilon \sim 0.1\ \rm M^{-1}{\cdot}cm^{-1}$) absorption band at around 245–255 nm, corresponding to the resonance excitation to ^6D_J levels. The ratio is then calculated to be ∼0.1001 using these moderate absorption lines, resulting in a systematic error of as small as 0.1%. Above ^6D_J levels are ^6G_J levels located near the wavenumber of $50\,000\ \rm cm^{-1}$ (resonance excitation wavelength of 200 nm) [3,18], but photons at such short wavelengths are easily absorbed by water [19], and thus excited levels higher than ^6D_J levels are considered to contribute little to the Gd^{3+} emission BG. In this work, an aqueous solution of Gd sulfate was irradiated with a tunable pulsed laser at $\lambda_{\rm ex} = 245$–255 nm to observe the emission of Gd^{3+} ions at 312 nm, as shown in Fig. 2. From the obtained excitation spectrum, the spectral widths of resonant peaks and $\epsilon_{\rm DC}$ at non-resonant wavelengths shorter than the emission wavelength were estimated, which were then assumed in the simulation study to evaluate the Gd^{3+} emission BG at the SK-Gd detector.

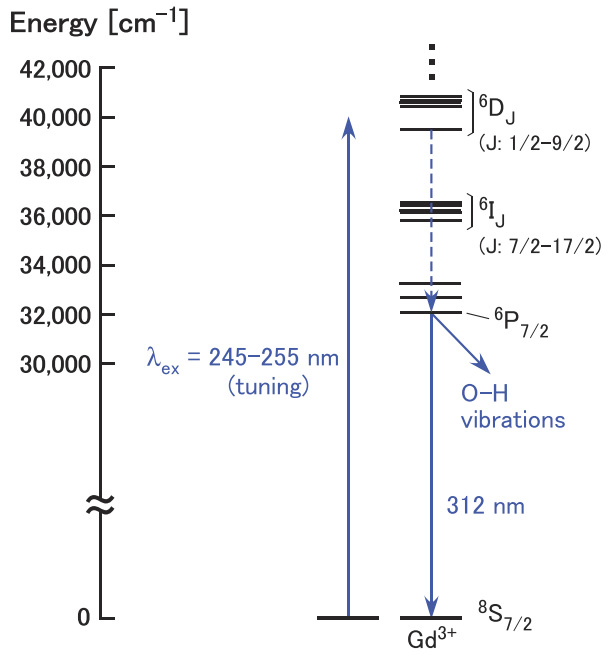

Fig. 2. Excitation and emission schemes of Gd^{3+} ion in this study.

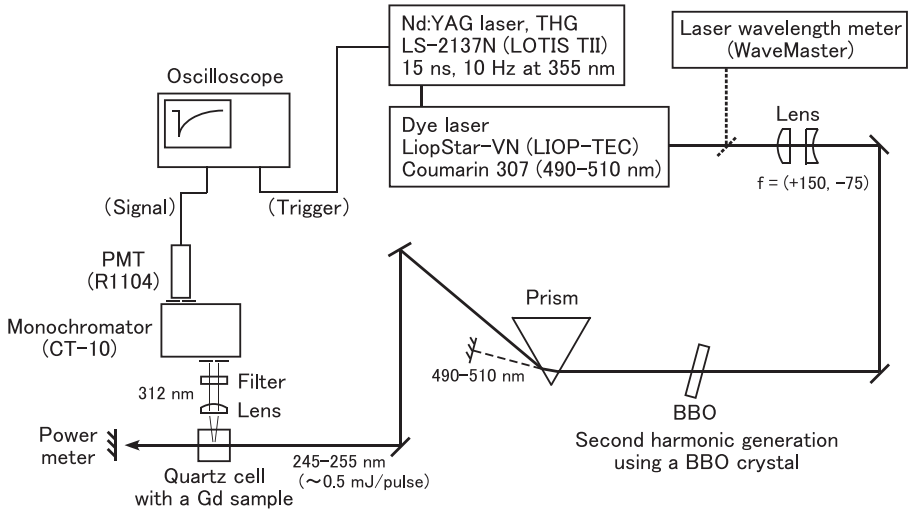

Fig. 3. Experimental setup for the emission measurement of Gd^{3+} ions.

3. Emission measurement of the Gd^{3+} ion

3.1. *Experimental setup*

Figure 3 shows our experimental setup based on time-resolved laser-induced luminescence spectroscopy to investigate the emission characteristics of Gd^{3+} ions in water. The laser source for excitation was a LIOP-TEC LiopStar-VN tunable pulsed dye laser pumped by the third harmonic (355 nm) of a LOTIS TII LS-2137N Nd:YAG pulsed laser. The entire laser system was operated at a repetition rate of 10 Hz with approximately 15 ns pulse duration [20]. Coumarin 307 dye was used to generate a tunable pulsed laser in the wavelength range of 490–510 nm. The wavelength of the dye laser was measured with a Coherent WaveMaster laser wavelength meter with an accuracy of 0.005 nm [21]. The diameter of the output laser beam was adjusted

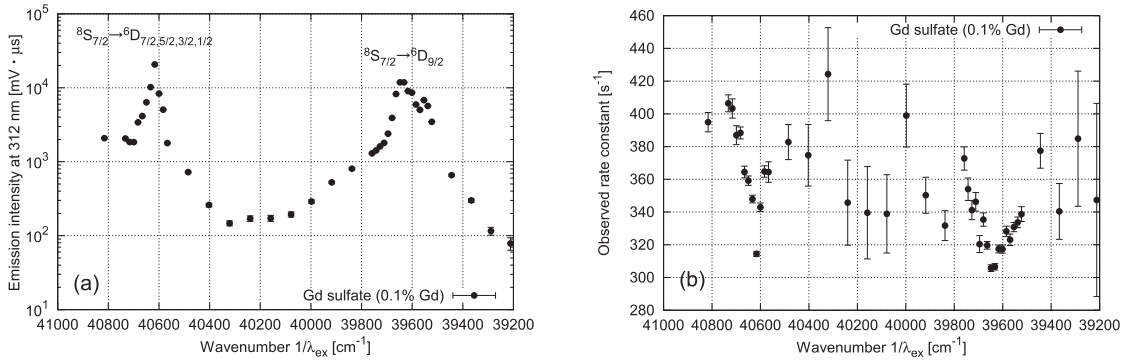

Fig. 4. Wavenumber ($1/\lambda_{ex}$) dependence of the measured (a) emission intensity and (b) rate constant ($1/\tau_{obs}$).

to about 2–3 mm using a pair of convex and concave lenses with focal lengths of $f = 150$ mm and $f = -75$ mm, respectively. A BBO crystal was used for second harmonic (245–255 nm) generation, which was separated from the fundamental (490–510 nm) beam by an equilateral dispersive prism and then introduced into a quartz cell ($L = 2$ cm) containing an aqueous solution sample of Gd sulfate to excite the Gd^{3+} ions. Since the wavelength conversion efficiency of coumarin 307 dye is dependent on the output wavelength (490–510 nm), the pump laser energy was adjusted so that the excitation laser output remained constant at around 0.5 mJ/pulse over the wavelength range of $\lambda_{ex} = 245$–255 nm. The linewidth of the excitation laser was less than 0.1 cm^{-1} (0.0006 nm at 250 nm) [22].

An aqueous solution sample of Gd sulfate was prepared by dissolving an appropriate amount of commercially available Gd sulfate (FUJIFILM Wako Pure Chemical 93-6407) in ultrapure water. In this study, three samples with Gd concentrations of 0.01%, 0.03%, and 0.1% were used.

The emission of Gd^{3+} ions at 312 nm was collimated using a convex lens with a focal length of $f = 50$ mm (Thorlabs LA4148-UV) and passed through a bandpass filter with a center wavelength of 313 ± 2 nm and an FWHM of 10 ± 2 nm (Edmund 34-977) to suppress the scattered light of the introduced laser beam. After further removing the scattered light using a monochromator (JASCO CT-10), which was also used to confirm the detection of Gd^{3+} ion emission at 312 nm by turning the dial, the Gd^{3+} emission was detected with a photomultiplier tube (PMT, Hamamatsu Photonics R1104). The PMT output signals were averaged 1024 times and recorded by an oscilloscope.

3.2. *Measurement results*

The excitation laser wavelength was tuned in the range of $\lambda_{ex} = 245$–255 nm. For each excitation wavelength, the averaged oscilloscope waveform was fitted by the following formula to obtain the emission intensity:

$$f(t) = V_0 \cdot \exp\left(-\frac{t - t_0}{\tau_{obs}}\right) + V_{BG}, \tag{3}$$

where the excitation laser was irradiated at $t = t_0$. Data points at $t \geq t_0 + 0.2$ ms were used for the fitting to remove scattered light noises. The emission intensity was determined by integrating net signal voltage over time, i.e., $\int_{t_0}^{\infty} |f(t) - V_{BG}|\, dt = |V_0| \cdot \tau_{obs}$. Figure 4 shows the wavenumber dependence of the measured (a) emission intensity and (b) rate constant $1/\tau_{obs}$.

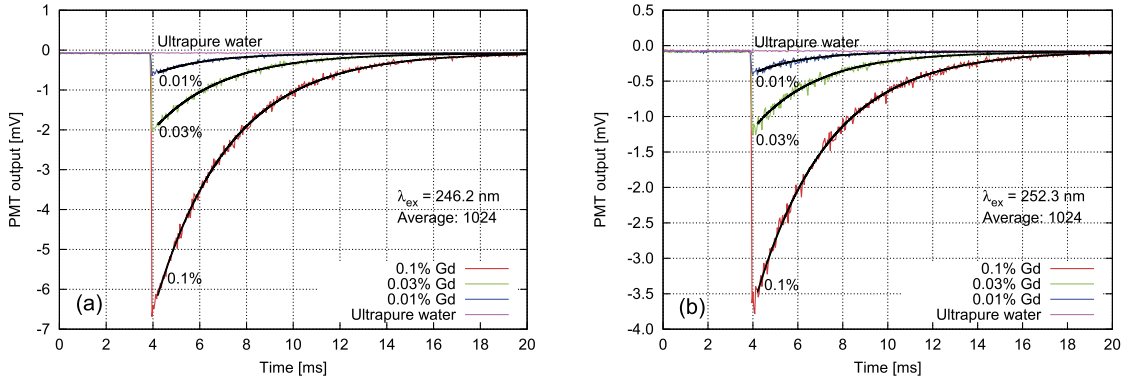

Fig. 5. Observed oscilloscope waveforms at (a) $\lambda_{ex} = 246.2$ nm and (b) $\lambda_{ex} = 252.3$ nm with exponential curves fitted on the waveforms for samples other than ultrapure water.

Since the wavenumber dependences are expected to be independent of the Gd concentration, we used a sample with a Gd concentration of 0.1% in these measurements to clearly observe the emission signals.

Large resonant peaks were observed at $\lambda_{ex} = 246.2$ nm (40 617 cm^{-1}) and 252.3 nm (39 635 cm^{-1}). The former corresponds to resonance excitation to one of the $^6D_{1/2}$, $^6D_{3/2}$, $^6D_{5/2}$, and $^6D_{7/2}$ levels; these four energy levels are close to each other [3]. The latter indicates resonance excitation to the $^6D_{9/2}$ level. Since multiple levels contribute to the former peak, the spectral widths (FWHMs) of resonant peaks were estimated from the latter peak shape to be of the order of 100 cm^{-1}. The linewidth (<0.1 cm^{-1}) of the excitation laser was sufficiently narrow to ensure that the observed spectral widths were attributed to the electronic structure of Gd^{3+} ions in the sample. A molar attenuation coefficient $\epsilon_{DC} \sim 0.001$ $M^{-1}\cdot cm^{-1}$ at non-resonant wavelengths shorter than the emission wavelength was estimated from the fact that the measured emission intensity at non-resonant wavelengths was two orders of magnitude lower than that at 252.3 nm, and that the molar attenuation coefficient for the $^6D_{9/2}$ level is $\epsilon \sim 0.1$ $M^{-1}\cdot cm^{-1}$ [13]. These spectral widths and ϵ_{DC} were assumed in the simulation study described in Sect. 4. The measured emission lifetimes τ_{obs} were around 3 ms. The error bars in Fig. 4 are fitting errors only, and repeated measurements under the same conditions did not show significant differences in the observed emission lifetimes τ_{obs} at $\lambda_{ex} = 245$–255 nm in this study. Note that the emission lifetime can be affected by quenching due to contamination during the preparation, storage, and measurement of Gd sulfate samples.

Figure 5 shows an example of the observed oscilloscope waveforms at (a) $\lambda_{ex} = 246.2$ nm and (b) $\lambda_{ex} = 252.3$ nm with sample conditions of 0.1% Gd (red), 0.03% Gd (green), 0.01% Gd (blue), and ultrapure water (purple). Exponential curves fitted on the waveforms for samples other than ultrapure water are also shown in the figure. The emission signals of Gd^{3+} ions were clearly observed with a Gd concentration down to 0.01% for both resonant wavelengths. The relationship between Gd concentration and fitted peak emission voltage $|V_0|$ is shown for each of $\lambda_{ex} = 246.2$ nm and 252.3 nm in Fig. 6. Here, $|V_0|$ was used instead of the emission intensity $|V_0| \cdot \tau_{obs}$ to avoid systematic uncertainties in emission lifetimes caused by quenching due to contamination mentioned above when handling different samples. In each measurement, the transmitted excitation laser output was recorded with a power meter (see Fig. 3), and the fitted peak emission voltages $|V_0|$ were normalized to those under the transmitted output of 0.5 mJ/pulse to compensate for variations (typically 10%) in the excitation laser output. The

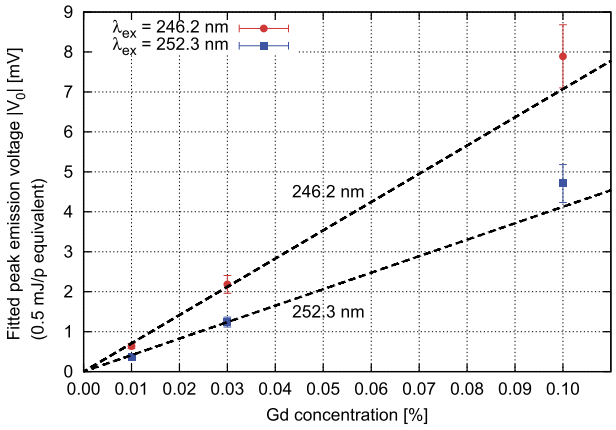

Fig. 6. Relationship between Gd concentration and fitted peak emission voltage for $\lambda_{ex} = 246.2$ nm and 252.3 nm.

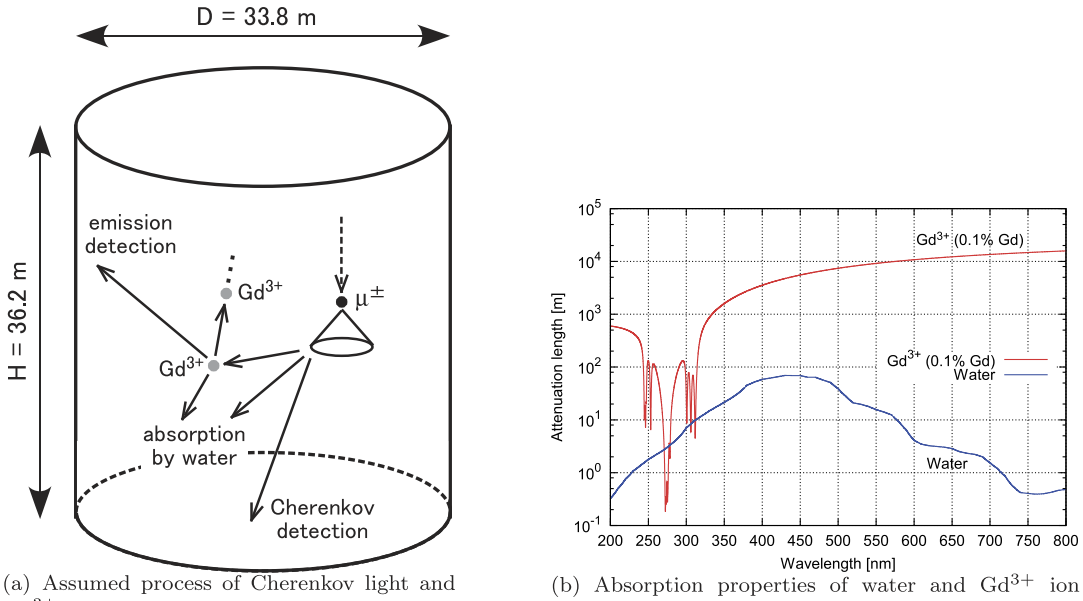

(a) Assumed process of Cherenkov light and Gd^{3+} emission detection

(b) Absorption properties of water and Gd^{3+} ion (0.1% Gd)

Fig. 7. Simulation overview.

error bars in this figure represent both the statistical error obtained by repeating the same measurement five times and the systematic uncertainty of ∼10% in the observed emission signals in each condition. A linear fit to the data is also shown for each of $\lambda_{ex} = 246.2$ nm and 252.3 nm. In general, good linearity was observed between Gd concentration and fitted peak emission voltage $|V_0|$ (and hence emission intensity) for both resonant wavelengths, indicating that our setup is useful for remote monitoring of Gd concentration in the SK-Gd project without the need to collect solution samples from the sampling port.

4. Simulation study

4.1. *Simulation conditions*

To estimate the influence of the Gd^{3+} emission BG on the observation of electron antineutrino events, a simulation study was performed assuming the geometry of the SK-Gd detector [23], as shown in Fig. 7(a). Simulation conditions are summarized in Table 1, which are also briefly

Table 1. List of simulation conditions.

Water tank	Tank size: 33.8 m in diameter and 36.2 m in height (ID) [23]
Cherenkov photon	Position: uniform generation in the tank Direction: angle $\theta = \cos^{-1}(1/1.33)$ from vertically downward Wavenumber: uniform in the range of 12 500–50 000 cm^{-1} (i.e., $\propto 1/\lambda^2$ in the wavelength range of 200–800 nm)
Absorption by water	Absorption coefficients: reference values [19]
Gd concentration	0.01%, 0.03%, or 0.1%
Absorption by Gd^{3+} ion	Spectroscopic data: Table 2
Gd^{3+} emission	$^6P_{7/2} \rightarrow {}^8S_{7/2}$ at 312 nm only Lifetime: $\tau_{rad} = 10.9$ ms [13], and $\tau_{obs} = 1,\ 3,$ or 10 ms
Detection criteria	Cherenkov photon: reach the tank wall without being absorbed by water or Gd^{3+} ions Gd^{3+} emission: Cherenkov photon absorbed by a Gd^{3+} ion, and the subsequent Gd^{3+} emission to reach the tank wall without being absorbed by water or quenched by O–H vibrations etc.
PMT quantum efficiency	SK data [23]
Normalization	SK data: typically $\sim 10^5$ pe generated by Cherenkov photons from a cosmic muon event [23,24]

described as follows. Cherenkov photons from a cosmic muon event were generated uniformly in the SK inner detector (ID). They traveled in the direction of angle $\theta = \cos^{-1}(1/1.33)$ from vertically downward, where 1.33 is the refractive index of water. Due to significant absorption by water and low sensitivity of PMTs at wavelengths of shorter than 200 nm or longer than 800 nm, the wavelength distribution of Cherenkov photons was here proportional to $1/\lambda^2$ in the range of 200–800 nm, meaning a uniform wavenumber distribution in the range of 12 500–50 000 cm^{-1}.

As shown in Fig. 7(a), some of the Cherenkov photons were absorbed by water or Gd^{3+} ions; the remaining ones were detected when they reached the tank wall. Reference values and measurement results described in Sect. 3 were used for the absorption properties of water [19] and the Gd^{3+} ion [3,13] (see Fig. 7(b) and Table 2). Molar attenuation coefficients for the ^6P_p ($p = 3/2,\ 5/2$) and ^6D_d ($d = 1/2,\ 3/2,\ 5/2,\ 7/2$) levels in Table 2 were determined based on the statistical weight of each level. For the wavelength dependence of the PMT quantum efficiency, data published by SK [23] were used. In this simulation, the photon coverage was not considered because it was canceled out by using the normalization that $\sim 10^5$ photoelectrons (pe) were generated by Cherenkov photons from a typical cosmic muon event [23,24].

Once Cherenkov photons were absorbed by Gd^{3+} ions, they resulted in emission ($^6P_{7/2} \rightarrow {}^8S_{7/2}$) at 312 nm or quenching by O–H vibrations etc. The former emitted photons could be absorbed by other Gd^{3+} ions followed by the same emission or quenching as well, and they were finally detected when they reached the tank wall without being absorbed by water or quenched by O–H vibrations etc. We calculated the time dependence of the expected pe count rate resulting from the Gd^{3+} emission under Gd concentrations of 0.01%, 0.03%, and 0.1%, and under the observed lifetimes (τ_{obs}) of 1 ms, 3 ms, and 10 ms.

4.2. *Simulation results*

Figure 8 shows the calculated time dependence of the expected pe count rate under $\tau_{obs} = 1,\ 3,$ and 10 ms with a Gd concentration of 0.01%. An exponential fit to the data for each τ_{obs}

Table 2. Assumed spectroscopic data of Gd^{3+} ions in the simulation study.

Level	Energy [cm^{-1}]	Molar attenuation coefficient ϵ [$M^{-1}\cdot cm^{-1}$]	FWHM [cm^{-1}]
$^6P_{3/2}$	33 262 [3]	0.15 × 4/8	
$^6P_{5/2}$	32 680 [3]	0.15 × 6/8	
$^6P_{7/2}$	32 084 [3]	∼0.15 [13]	
$^6I_{7/2}$	35 920 [13]	0.29 [13]	
$^6I_{9/2}$	36 258 [13]	0.92 [13]	
$^6I_{11/2}$	36 536 [13]	1.38 [13]	
$^6I_{13/2}$	36 576 [13]	1.22 [13]	100
$^6I_{15/2}$	36 710 [13]	3.41 [13]	
$^6I_{17/2}$	36 337 [13]	2.00 [13]	
$^6D_{1/2}$	40 444 [3]	0.1 × 2/10	
$^6D_{3/2}$	40 694 [3]	0.1 × 4/10	
$^6D_{5/2}$	40 857 [3]	0.1 × 6/10	
$^6D_{7/2}$	40 599 [3]	0.1 × 8/10	
$^6D_{9/2}$	39 508 [3]	∼0.1 [13]	
DC	32 084–50 000	0.001	–

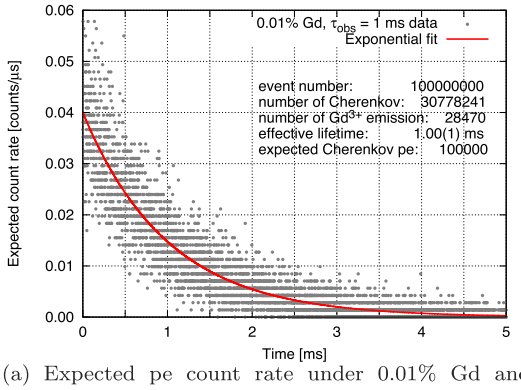

(a) Expected pe count rate under 0.01% Gd and $\tau_{obs} = 1$ ms

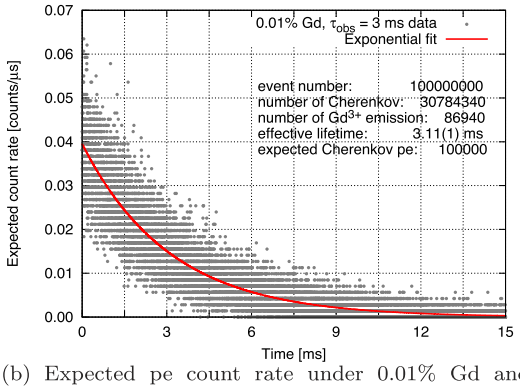

(b) Expected pe count rate under 0.01% Gd and $\tau_{obs} = 3$ ms

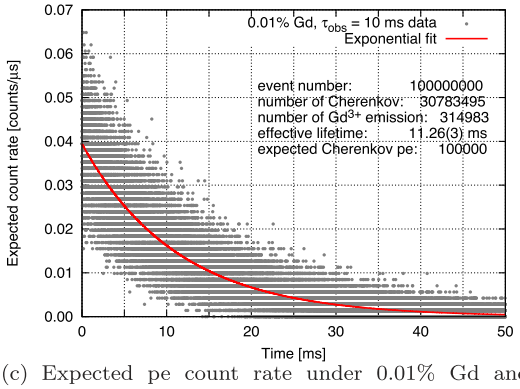

(c) Expected pe count rate under 0.01% Gd and $\tau_{obs} = 10$ ms

Fig. 8. Simulation results for a Gd concentration of 0.01%.

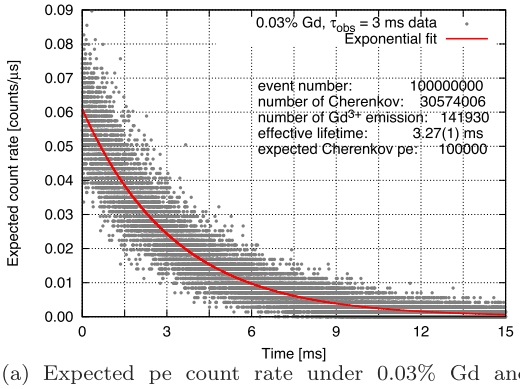

(a) Expected pe count rate under 0.03% Gd and $\tau_{obs} = 3$ ms

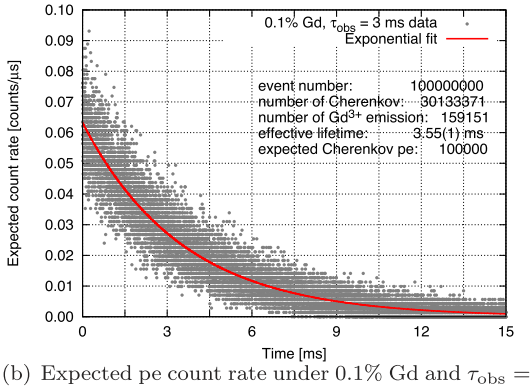

(b) Expected pe count rate under 0.1% Gd and $\tau_{obs} = 3$ ms

Fig. 9. Simulation results for an observed lifetime of 3 ms.

condition is also shown to evaluate the effective lifetime of Gd^{3+} emission. Particularly in the case of long τ_{obs}, the effective lifetime was slightly longer than the assumed τ_{obs}, which reflects the reabsorption of Gd^{3+} emission by other Gd^{3+} ions. Although the detection probability of Gd^{3+} emission depended on the assumed τ_{obs}, the expected pe count rate immediately after the cosmic muon event ($t = 0$ ms) remained almost constant at ~0.04 counts/μs.

Figure 9 shows the calculated time dependence of the expected pe count rate under Gd concentrations of 0.03% and 0.1% with $\tau_{obs} = 3$ ms. The expected pe count rate at $t = 0$ ms increased by about 1.6 times when increasing the Gd concentration from 0.01% to 0.03%, but it increased only slightly from 0.03% to 0.1%. Higher concentrations of Gd resulted in large absorption of Cherenkov photons, and increased quenching due to reabsorption of Gd^{3+} emission as well. According to the simulation results, the Gd^{3+} emission BG rate from cosmic muons is expected to be 10^{-1} counts/μs or less with a Gd concentration up to 0.1%, which seems small but not negligible. Our calculation results mentioned above depend on the following Gd^{3+} spectroscopic parameters (assumed in this study): radiative lifetime τ_{rad} (10.9 ms), molar attenuation coefficients ϵ_i at resonant wavelengths λ_i with their FWHMs (Table 2), and molar attenuation coefficient ϵ_{DC} at non-resonant wavelengths shorter than the emission wavelength (0.001 $M^{-1}\cdot cm^{-1}$). Improving the accuracy of these parameters will be helpful for more precise evaluation of the Gd^{3+} emission BG at the SK-Gd detector.

5. Conclusion

The SK-Gd project is ongoing, where Gd sulfate is dissolved in a water Cherenkov detector to increase the detection sensitivity of supernova relic neutrino events. As a possible BG source for the detection of Cherenkov signals, investigation of the emission characteristics of Gd^{3+} ions in water is essential. In this work, an experimental setup based on time-resolved laser-induced luminescence spectroscopy was constructed where the excitation laser wavelength was tuned in the range of 245–255 nm to excite Gd^{3+} ions to around ^6D_J levels. Large resonant peaks were observed at $\lambda_{ex} = 246.2$ nm (40 617 cm^{-1}) and 252.3 nm (39 635 cm^{-1}), with the latter peak FWHM being of the order of 100 cm^{-1}. By comparing the measured emission intensities at resonant and non-resonant wavelengths, the molar attenuation coefficient at non-resonant wavelengths shorter than the emission wavelength was estimated to be $\epsilon_{DC} \sim 0.001$ $M^{-1}\cdot cm^{-1}$. The measured emission lifetimes were $\tau_{obs} \sim 3$ ms, little dependent on the excitation laser wavelength in the range of 245–255 nm. Good linearity was observed in the relationship between

Gd concentration and emission intensity for both resonant wavelengths, indicating that our setup is useful for the remote monitoring of Gd concentration in the SK-Gd project. According to the simulation results assuming the geometry of the SK-Gd detector, a high concentration of Gd resulted in only a slight increase in emission intensity because of large absorption of Cherenkov photons and increased quenching due to reabsorption of Gd^{3+} emission as well. The expected Gd^{3+} emission BG rate from cosmic muons is $\sim 10^{-1}$ counts/μs or less with a Gd concentration up to 0.1%, which seems small but not negligible. Improving the accuracy of Gd^{3+} spectroscopic data will be helpful for more precise evaluation of the Gd^{3+} emission BG at the SK-Gd detector.

Acknowledgements

This study was partially supported by JSPS KAKENHI Grant Number JP19H05808, and by the Inter-University Research Program of the Institute for Cosmic Ray Research (ICRR), the University of Tokyo.

REFERENCES

[1] G. Blasse, Phys. Status Solidi A **130**, K85 (1992).
[2] Z. Wang, T. Senden, and A. Meijerink, J. Phys. Chem. Lett. **8**, 5689 (2017).
[3] V. A. Dzuba, O. P. Sushkov, W. R. Johnson, and U. I. Safronova, Phys. Rev. A **66**, 032105 (2002).
[4] S. Chandrasekaran, P. Basu, H. Krishnan, K. Sivasubramanian, R. Baskaran, and B. Venkatraman, Prog. Nucl. Energy **107**, 57 (2018).
[5] J. F. Beacom and M. R. Vagins, Phys. Rev. Lett. **93**, 171101 (2004).
[6] L. Marti et al., Nucl. Instrum. Meth. A **959**, 163549 (2020).
[7] K. Abe et al., Nucl. Instrum. Meth. A **1027**, 166248 (2022).
[8] A. Tang, G. H. Smith, V. A. Kudryavtsev, and A. Tonazzo, Phys. Rev. D **74**, 053007 (2006).
[9] M. Shinoki, The Super-Kamiokande Collaboration, J. Phys.: Conf. Ser. **2156**, 012187 (2022).
[10] J.-C. G. Bünzli and S. V. Eliseeva, Basics of lanthanide photophysics, in Lanthanide Luminescence (Springer, Berlin, 2010), Springer Series on Fluorescence, Vol. 7, p. 1.
[11] S. Lis, T. Kimura, and Z. Yoshida, J. Alloys Compd. **323-324**, 125 (2001).
[12] T. Kimura, R. Nagaishi, Y. Kato, and Z. Yoshida, Radiochim. Acta **89**, 125 (2001).
[13] W. T. Carnall, The absorption and fluorescence spectra of rare earth ions in solution, in Handbook on the Physics and Chemistry of Rare Earths, eds. K. A. Gschneidnerand L. Eyring (North-Holland Publishing Company,Amsterdam, 1979), Chap. 24.
[14] J.-J. Vuilleumier, M. Deschaux, and M. D. Marcantonatos, J. Chem. Soc. Faraday Trans. 1 **85**, 2605 (1989).
[15] L. Z. Jiao, D. M. Dong, W. G. Zheng, W. B. Wu, H. K. Feng, C. J. Shen, and H. Yan, Asian J. Chem. **25**, 2273 (2013).
[16] L. A. Szolga and T. R. Cilean 2020 International Conference on e-Health and Bioengineering (EHB). Nitrates and Nitrites Detection System in the Drinking Water Using UV Absorption (2020).IEEE.
[17] J. S. Gaffney, N. A. Marley, and M. M. Cunningham, Environ. Sci. Technol. **26**, 207 (1992).
[18] R. T. Wegh and A. Meijerink, Acta Phys. Polon. A **90**, 333 (1996).
[19] R. C. Smith and K. S. Baker, Appl. Opt. **20**, 177 (1981).
[20] LOTIS TII, Specification. LOTIS TII. (2022) [Date of access: May 11, 2022].https://lotis-tii.com/ls-2137nmh-ls-2147nmh.
[21] Coherent, WaveMaster User Manual. Coherent.(2013) [Date of access: April 28, 2022]. https://content.coherent.com/legacy-assets/pdf/WaveMaster-User-Manual_FORMFIRST.pdf.
[22] LIOP-TEC, Pulsed Dye Laser LIOPSTAR & LIOPSTAR-E. LIOP-TEC. (2014) [Date of access: May 9, 2022].http://www.liop-tec.com/resources/LiopStar-complete+2014.pdf.
[23] S. Fukuda et al., Nucl. Instrum. Meth. A **501**, 418 (2003).
[24] K. Abe et al., Nucl. Instrum. Meth. A **737**, 253 (2014).